Journal of Vibration Engineering & Technologies (2022) 10:1399–1412
https://doi.org/10.1007/s42417-022-00454-7

ORIGINAL PAPER

# Longitudinal Vibration Analysis of a Stepped Nonlocal Rod Embedded in Several Elastic Media

**Moustafa S. Taima[1] · Tamer El-Sayed[1,2,3] · Said H. Farghaly[1]**

Received: 21 November 2021 / Revised: 21 November 2021 / Accepted: 1 March 2022 / Published online: 28 March 2022


## Abstract

**Purpose** Mechanical properties of 1D nanostructures are of great importance in nanoelectromechanical systems (NEMS) applications. The free vibration analysis is a non-destructive technique for evaluating Young's modulus of nanorods and for detecting defects in nanorods. Therefore, this paper aims to study the longitudinal free vibration of a stepped nanorod embedded in several elastic media.

**Methods** The analysis is based on Eringen's nonlocal theory of elasticity. The governing equation is obtained using Hamilton's principle and then transformed into the nonlocal analysis. The dynamic stiffness matrix (DSM) method is used to assemble the rod segments equations. The case of a two-segment nanorod embedded in two elastic media is then deeply investigated.

**Results** The effect of changing the elastic media stiffness, the segments stiffness ratio, boundary conditions and the nonlocal parameter are examined. The nano-rod spectrum and dispersion relations are also investigated.

**Conclusion** The results show that increasing the elastic media stiffness and the segment stiffness ratio increases the natural frequencies. Furthermore, increasing the nonlocal parameter reduces natural frequencies slightly at lower modes and significantly at higher modes.

**Keywords** Nanorod · Stepped rod · Exact solution · Elastic Media · Continuum mechanics · Dynamic stiffness matrix

## Abbreviations

| | |
|---|---|
| $a$ | Internal characteristic length |
| $A_j$ | Cross-sectional area of jth segment |
| $A_{j1}$ | $\frac{A_j}{A_1}$ |
| $C_{1_j}, C_{2_j}$ | Constants |
| $C_{ijkl}$ | Elastic modulus tensor |
| $\mathbf{D}$ | Overall DSM |
| $\mathbf{D}_j$ | DSM of $j$th segment without attachments |
| $e_0$ | Calibration parameter |
| $\epsilon_{kl}$ | Strain tensor |
| $E_j$ | Young's modulus of $j$th segment |
| $E_{j1}$ | $\frac{E_j}{E_1}$ |
| $\mathbf{F}_j$ | Forces vector |
| $J$ | Segments number |
| $J+1$ | Nodes number |
| $K_j$ | Elastic media stiffness of $j$thsegment |
| $\bar{K}_1$ | Dimensionless elastic media stiffness of 1st segment |
| $K_{j1}$ | $\frac{K_j}{K_1} = \frac{\bar{K}_j}{\bar{K}_1}$ |
| $K_{s_1}$, $K_{s_{J+1}}$ | Linear spring stiffness at left and right end |
| $\bar{K}s_1$ , $\bar{K}s_{J+1}$ | Dimensionless stiffness at left and right end |
| $l$ | External characteristic length |
| $l_j$ | $\frac{L_j}{L}$ dimensionless length of $j$th segment |
| $L$ | Total length of the rod |
| $L_j$ | Length of $j$thsegment |
| $m_j$ | $\rho_j A_j$ mass per unit length of $j$th segment |
| $N_j$ | Axial force per unit length of $j$thsegment |
| $\mathbf{S}$ | Attachments matrix |
| $t$ | Time |
| $u_j(x,t)$ | Axial displacement of $j$thsegment |

✉ Tamer El-Sayed
tamer.el-sayed@abdn.ac.uk

Moustafa S. Taima
moustafa.samir@m-eng.helwan.edu.eg

Said H. Farghaly
said.farghaly@m-eng.helwan.edu.eg

[1] Department of Mechanical Design, Faculty of Engineering, Mataria, Helwan University, P.O. Box 11718, Helmeiat-Elzaton, Cairo, Egypt

[2] Centre for Applied Dynamics Research, School of Engineering, University of Aberdeen, Aberdeen AB24 3UE, UK

[3] School of Engineering, University of Hertfordshire Hosted by Global Academic Foundation, Cairo, Egypt

| | |
|---|---|
| $\mathbf{U}_j$ | Displacement vector of *j*th segment |
| $x$ | Axial coordinate |
| $X$ | Reference point |
| $X\prime$ | Any point in the body |
| $\Gamma_j$ | Kinetic energy of *j*thsegment |
| $\varepsilon_{xx}$ | Strain in x direction |
| $\zeta$ | Nonlocal parameter |
| $\xi_j$ | $\frac{x_j}{L_j}$ dimensionless axial coordinate |
| $\Pi_j$ | Potential energy of *j*th segment |
| $\rho_j$ | mass density of *j*th segment |
| $\rho_{j1}$ | $\frac{\rho_j}{\rho_1}$ |
| $\sigma_{ij}$ | Stress tensor |
| $\sigma_{ij}^c$ | Classical stress tensor |
| $\sigma_{xx}$ | Stress in *x* direction |
| $\varphi$ | Kernel function |
| $\omega$ | Circular frequency |
| $\Omega_{1_{(n)}}$ | Dimensionless natural frequency $\sqrt{\frac{\rho_1\omega^2L^2}{E_1A_1}}$ |
| $\nabla^2$ | Second-order spatial gradient |

## Introduction

Recently, researchers have shown an increased interest in nanostructures due to their extraordinary properties. High strength, good thermal and electrical properties are some of the properties of nanostructures [1]. Nanostructures have many technological applications, such as, micro and nano electromechanical systems (MEMs and NEMs). In order to develop an accurate design of nanostructures, it is important to understand their behavior.

Nanorods, nanobeams and nanowires are examples of 1D nanostructures. One of the popular nanostructures is carbon nanotubes (CNTs) were discovered by Iijima [2]. The vibrations of 1D nanostructures have recently received considerable attention due to their application in several nanotechnological instruments such as atomic force microscopy, nanomechanical cantilever sensors, etc. The natural frequency of 1D nanowires can be determined experimentally by driving these nanorods to their resonant frequency modes using mechanical or electrical methods. Then, by using vibration analysis, the nanowires Young's modulus can be evaluated. One of the advantages of this method is that it is nondestructive .

The vast research in nanostructures may be classified into two main categories [1]: the experimental methods and the analytical modeling. The experimental methods are a possible way to investigate nanostructures [3], although the experimental methods are quite challenging because controlling every parameter in nanoscale is a complex task.

The analytical modeling category can be divided into two sub-groups: quantum mechanics and continuum mechanics. Quantum mechanics modelling may be grouped into the following categories: ab-initio method, density functional theory, Monte Carlo simulation, molecular mechanics and molecular dynamics. Molecular dynamics (MD) is one of the most popular quantum mechanics methods. Molecular dynamics is a simulation in the atomistic level [4]. Therefore, MD is time consuming, computationally expensive and not suitable for the analysis of nanostructures that consist of a large number of atoms and molecules [5].

Continuum mechanics, that is popular to engineers on its classical formulation, is used in nanostructures analysis [6]. In the classical continuum mechanics theory, the stresses at a point *X* depend on the strain at that point *X* only. The classical continuum theory requires some modifications at the nano scale because the size effect of the nanostructures has a great influence on its behavior [7].

In general, conventional continuum mechanics is a size effect-free theory. Therefore, much research is done to include the size effect into the classical continuum mechanics. This lead to many theories such as nonlocal elasticity theory, modified coupled stress theory, surface energy methods, multiscale models, and hybrid methods. In the current work, the analysis is based on nonlocal continuum elasticity theory [8]. In the nonlocal elasticity theory, the stress at a point *X* is a function of strain at that point *X* and all nearby points *X′* in the continuum [9]. Eringen theory is simple in deriving the equations and analysis of nanostructures. It is also worth noting that this theory can be divided into integral-based and differential-based models. A large number of studies investigated the static analysis [10], buckling [11]and vibration [12–14] of nanostructure using nonlocal continuum mechanics.

The longitudinal vibration of nanorod are studied using different analysis methods and parameters by many researchers. Aydogdu [15] studied the axial vibration of nanorod for clamped–clamped (C–C) and clamped–free (C–F) boundary conditions. Huang [16] examined the nonlocal long-range influence on the axial vibration of nanorod. Aydogdu [17] examined the effect of various parameters like C–C and C–F boundary conditions and the stiffness of the elastic medium. Adhikari et al. [18] investigated the free and forced axial vibration for nanorod using the dynamic finite element analysis. Demir and Civalek [19] examined the size effect on a continuous and discrete non-local models. They studied both the torsional and axial vibration analysis of microtubules. Güven [20] studied the longitudinal vibration of nano-rod using nonlocal strain gradient elasticity theory. The lateral deformation and shear strain effects are included by using the Love rod model and Bishop's correction. Adhikari et al. [21] used the dynamic finite element method to investigate a nanorod embedded in an elastic medium. They used conventional and dynamic finite elements methods for obtaining the dynamic response for the rod.

Gul et al. [22] used doublet mechanics to investigate C–C and C–F carbon nanotube embedded in an elastic media. Numanoğlu et al. [23] presented the effect of nonlocal parameter, boundary conditions, attachments and length on the axial vibration behavior of nanorod using Eringen's nonlocal theory. Loghmani et al. [24] analysed the free axial vibration of several cracked, stepped nanorod with attached mass at the tip of the rod. Ebrahimi et al. [25] investigated static stability and vibration analysis of a functionally graded nanobeams. The analysis is based on nonlocal theory of elasticity and modified couple stress theory to capture the size effects accurately. Civalek et al. [26] analyzed the lateral and axial vibration of embedded nanobeams based on Eringen's theory using finite element method. Yayli [27] used Eringen's theory to investigate the axial vibration of Rayleigh nanorod which is attached to axial elastic springs at both ends.

In an exact solution of multi-span rod or beams, the boundary conditions and the intermediate conditions of each segment are derived [28, 29]. Then these equations are assembled. There are several methods to assemble the segments equations but the most common methods are numerical assembly technique (NAT) [30, 31], transfer matrix method (TMM) [32, 33] and DSM [34–36]. In the current manuscript, DSM method is adopted.

In the majority of studies, vibrations are described as a linear combination of a structure's modes. Another way to describe vibrational phenomena is to think of vibrations as moving waves along structures. Media with various material characteristics and cross-section areas usually have different impedances. Many researchers have investigated impedance mismatch in solid structures [37–40]. Both descriptions frequently provide complementary views for vibrational analysis and this was considered in the first verification example.

From the previous literature and to the best of author's knowledge, there is no single study which dealt with vibration of a stepped nonlocal rod embedded in several elastic media using DSM method. Therefore, the primary purpose of the current work is to fill this gap by solving such problem. The rest of the paper is organized as follows: in Sect. 2, a brief overview on the nonlocal Eringen's theory is explained. Then the equation of motion is derived in the local formulation using Hamilton's method. Also, the local formulation for equation of motion is transformed to the nonlocal formulation using nonlocal Eringen's theory. In Sect. 3, the DSM method is used for the analysis. The case of two-segment nanorod embedded in two elastic media is introduced and the verification results are presented and validated with the published results in Sect. 4. In addition, the results for a C–C and C–F boundary conditions are introduced and discussed. Finally, the conclusion of the study is given in Sect. 5.

## The Nonlocal Mathematical Model

### A Brief Overview on the Nonlocal Elasticity Theory

The constitutive equations of linear, homogeneous, isotropic and nonlocal elastic solid with zero body forces are given by Eringen [41]. The stress tensor is defined by the integro-partial differential equation as:

$$\sigma_{ij}(X) = \int_{\Omega} \varphi(|X' - X|, \zeta)\sigma_{ij}^{c}(X')\, \mathrm{d}\Omega(X'), \tag{1}$$

where $\sigma_{ij}$ and $\sigma_{ij}^{c}$ are the stress tensor and classical stress tensor, respectively. $X$ is a reference point,$X'$ is any point in the body and $\varphi\ (|X' - X|, \zeta)$ denotes the nonlocal kernel function. The kernel function $\varphi$ depends on the distance between the points $X$ and $X'$ and the nonlocal parameter $\zeta = \frac{e_0 a}{\ell}$. The parameters $a$ and $\ell$ are the internal and external characteristic lengths, respectively. The parameter $e_0$ is used to calibrate the results of the nonlocal model to the atomic model. However, the identification of the small scaling parameter $e_0$ has not been fully understood. Several researchers reported several values for this parameter and these values are found to have a large scatter [9].

The integro-partial differential Eq. (1) is simplified to partial differential equation as:

$$\left(1 - \zeta^2 \ell^2 \nabla^2\right)\sigma_{ij}(x) = \sigma_{ij}^{c}(x) = C_{ijkl}\varepsilon_{kl}(x), \tag{2}$$

where $C_{ijkl}$ is elastic modulus tensor, $\varepsilon_{kl}$ is strain tensor and $\nabla^2$ denotes the second order spatial gradient. The nonlocal constitutive relation for 1D structures can be written as:

$$\sigma_{xx} - \left(e_0 a\right)^2 \frac{\mathrm{d}^2 \sigma_{xx}}{\mathrm{d}x^2} = E\varepsilon_{xx}. \tag{3}$$

### Equation of Motion in the Classical Form

A schematic representation for stepped nanorod embedded in several elastic media is shown in Fig. 1. The total length of the rod is $L$, that has $J$ segments and $J + 1$ nodes. The rod is constrained from the left and right sides by linear springs with stiffness $K_{s1}$, $K_{sJ+1}$ respectively. The axial coordinate is $x_j$ and the axial displacement is $u_j$. $E_j, \rho_j, L_j$, $A_j$ and $K_j$ are the Young's modulus, density, length, area and the surrounded elastic media stiffness of $j$th segment respectively. The stress concentration at each step is neglected during the present work.

The equation of motion of $j$th segment can be obtained using Hamilton's principle, which can be written as:

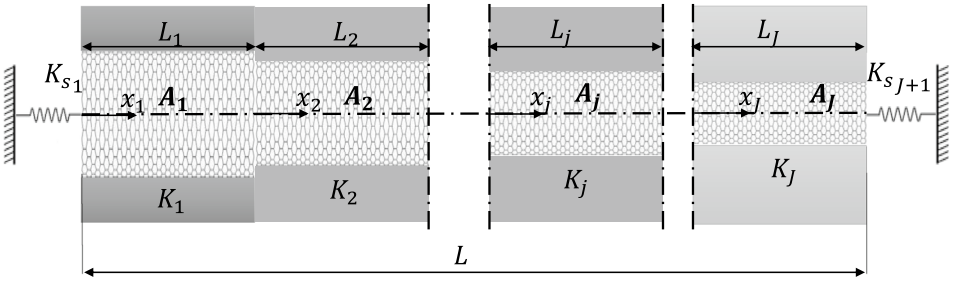


**Fig. 1** Stepped nanorod embedded in several elastic media

$$\mathbb{H}_j = \delta\left[\int_{t_1}^{t_2} \left(\Pi_j - \Gamma_j\right) \mathrm{d}t\right] = 0, \tag{4}$$

where $\delta$ is the variational symbol, $\Pi_j$ is the potential or strain energy and $\Gamma_j$ is the kinetic energy of $j$th segment.

The axial displacement and strain fields of $j$th segment are given by:

$$u_j = u_j(x,t), \quad \epsilon_j = \frac{\partial u_j}{\partial x}. \tag{5}$$

The kinetic and potential energies of $j$th segment embedded in elastic medium can be expressed as:

$$\Gamma_j = \frac{1}{2}\int_0^{L_j} m_j \left(\frac{\partial u_j}{\partial t}\right)^2 \mathrm{d}x_j, \tag{6}$$

$$\Pi_j = \frac{1}{2}\int_0^{L_j} \left[E_j A_j \left(\frac{\partial u_j}{\partial x}\right)^2 + K_j u_j^2\right] \mathrm{d}x_j, \tag{7}$$

where $m_j$ is the mass per unit length of $j$th segment. Substituting Eqs. (6, 7) in Hamilton's Eq. (4) gives:

$$\begin{aligned}\int_0^{L_j}\int_{t_1}^{t_2} &\left[E_j A_j \left(\frac{\partial u_j}{\partial x_j}\right)\delta\left(\frac{\partial u_j}{\partial x_j}\right)\right.\\ &\left. + K_j u_j \delta\left(u_j\right) - m_j\left(\frac{\partial u_j}{\partial t}\right)\delta\left(\frac{\partial u_j}{\partial t}\right)\right]\mathrm{d}x_j\mathrm{d}t = 0.\end{aligned} \tag{8}$$

Thus, the equation of motion of $j$th segment is obtained as:

$$K_j u_j + m_j \frac{\partial^2 u_j}{\partial t^2} = E_j A_j \frac{\partial^2 u_j}{\partial x_j^2} \quad \text{for every } \ 0 < x_j < L_j. \tag{9}$$

The axial force per unit length ($N_j$) of $j$th segment is expressed as:

$$N_j = E_j A_j \frac{\partial u_j}{\partial x_j}. \tag{10}$$

By differentiating Eq. (10) with respect to $x_j$ and substituting into Eq. (9), one can get:

$$\frac{\partial N_j}{\partial x_j} = K_j u_j + m_j \frac{\partial^2 u_j}{\partial t^2}. \tag{11}$$

## Equation of Motion in the Nonlocal Form

The nonlocal constitutive equation of $j$th segment can be obtained from Eqs. (3, 10) as follows

$$N_j - \left(e_0 a\right)^2 \frac{\partial^2 N_j}{\partial x^2} = E_j A_j \frac{\partial u_j}{\partial x_j}. \tag{12}$$

Equations (11, 12) can be used to obtain the nonlocal equation of motion and the axial forces of $j$th segment

$$\begin{aligned}K_j u_j + m_j \frac{\partial^2 u_j}{\partial t^2} &- \left(e_0 a\right)^2 K_j \frac{\partial^2 u_j}{\partial x_j^2}\\ &- \left(e_0 a\right)^2 m_j \frac{\partial^4 u_j}{\partial x_j^2 \partial t^2} = E_j A_j \frac{\partial^2 u_j}{\partial x_j^2},\end{aligned} \tag{13}$$

$$N_j = \left[E_j A_j + \left(e_0 a\right)^2 \left(m_j \frac{\partial^2}{\partial t^2} + K_j\right)\right]\frac{\partial u_j}{\partial x_j}. \tag{14}$$

The partial differential equation in Eq. (13) can be solved using the separation of variables method as:

$$u_j\left(x_j, t\right) = \hat{u}_j\left(x_j\right) T(t), \tag{15}$$

where $T(t) = \mathrm{e}^{\mathrm{i}\omega t}$, $\omega$ is the circular frequency and $\mathrm{i}^2 = -1$.

Substituting Eq. (15) into Eqs. (13) and (14) and transforming them into dimensionless form as:

$$\frac{E_j A_j - \left(e_0 a\right)^2 \left(m_j\,\omega^2 - K_j\right)}{L_j^2} U_j'' + (m_j\omega^2 - K_j) U_j = 0, \tag{16}$$

$$N_j\left(\xi_j\right) = \frac{E_j A_j - \left(e_0 a\right)^2 \left(m_j \omega^2 - K_j\right)}{L_j} U_j', \tag{17}$$

where $\xi_j = \frac{x_j}{L_j}, \hat{u}_j(x_j) = U_j(\xi_j)$ and $\frac{d\hat{u}_j}{dx_j} = \frac{1}{L_j}\frac{dU_j}{d\xi_j}$.

Equations (16) and (17) can be simplified by considering $E_{j1} = \frac{E_j}{E_1}$, $\rho_{j1} = \frac{\rho_j}{\rho_1}$, $l_j = \frac{L_j}{L}$, $K_{j1} = \frac{K_j}{K_1}$, and $A_{j1} = \frac{A_j}{A_1}$ as:

$$U_j'' + \alpha_j^2 U_j = 0, \tag{18}$$

$$N_j\left(\frac{L}{E_1A_1}\right) = \gamma_j U_j', \tag{19}$$

where $\alpha_j$ is the dimensionless wavenumber as shown below

$$\alpha_j = \sqrt{\frac{\frac{\rho_{j1}\ell_j^2}{E_{j1}}\Omega_1^2 - \frac{K_{j1}l_j^2}{E_{j1}A_{j1}}\bar{K}_1}{1-\mu^2(\frac{\rho_{j1}}{E_{j1}}\Omega_1^2 - \frac{K_{j1}}{E_{j1}A_{j1}}\bar{K}_1)}}, \tag{20}$$

and

$$\gamma_j = \frac{E_{j1}A_{j1}}{l_j}\left(1-\mu^2\left(\frac{\rho_{j1}}{E_{j1}}\Omega_1^2 - \frac{K_{j1}}{E_{j1}A_{j1}}\bar{K}_1\right)\right), \tag{21}$$

where $\Omega_1 = \sqrt{\frac{\rho_1 L^2\omega^2}{E_1}}$ and $\bar{K}_1 = \frac{K_1L^2}{E_1A_1}$ are the dimensionless frequency and stiffness of the 1st segment respectively and $\mu = \frac{e_0a}{L}$ is the dimensionless nonlocal parameter.

The solution of Eq. (18) is presented in terms of $C_{1_j}$ and $C_{2_j}$ as:

$$U_j(\xi_j) = C_{1_j}\, cos(\alpha_j\xi_j) + C_{2_j}\, sin(\alpha_j\xi_j). \tag{22}$$

The axial force may be expressed as:

$$N_j\left(\frac{L}{E_1A_1}\right) = \gamma_j\alpha_j(-C_{1_j}\sin(\alpha_j\xi_j) + C_{2_j}\, cos(\alpha_j\xi_j)). \tag{23}$$

## Wave Characteristics (Spectrum and Dispersion Relations)

In this section, the wave propagation concepts is used to determine the wave parameters, namely the wavenumber ($\alpha_j$) and the two different wave speeds (phase speed ($C_{ph}$) and group speed ($C_{gr}$)). From Eq. (20) the wave frequency is a function of the wavenumber $\alpha_j$, the nonlocal parameter $\mu$, the material property ($\rho_{j1}, E_{j1}$), rod geometry ($A_{j1}, l_j$), first elastic medium stiffness $\bar{K}_1$, and elastic media stiffness ratio ($K_{j1}$). If the wavenumber is real, the wave is said to be propagating. If the wavenumber is completely imaginary, the wave dampens out and is hence known to as evanescent mode. If wavenumber is complex, the wave will attenuate as it propagates. From Eq. (20), the propagating mode in this case is dispersive (i.e., the wave shape changes with propagation). In case of $\mu = 0$ and $\bar{K}_1 = 0$ the wavenumber becomes linearly proportional to wave frequency, which results in nondispersive propagating mode (i.e., the wave retains its shape as it propagates). In our case, the waves will not start propagating except after certain frequency called cut-off frequency ($\Omega_c$). The wavenumber before this frequency will be imaginary. For the present case the cut off frequency is obtained by setting $\alpha_j = 0$ as shown in Eq. (24). Moreover, the waves stop propagating after certain frequency called escape frequency ($\Omega_{es}$). The escape frequency is obtained by setting $\alpha_j$ tending to $\infty$ as shown in Eq. (25).

$$\Omega_c = \sqrt{\frac{K_{j1}\,\bar{K}_1}{\rho_{j1}\,A_{j1}}}, \tag{24}$$

$$\Omega_{es} = \sqrt{\frac{1+\mu^2\frac{K_{j1}}{E_{j1}A_{j1}}\bar{K}_1}{\mu^2\frac{\rho_{j1}}{E_{j1}}}}, \tag{25}$$

Then, the phase and group speeds should be determined. The phase speed is the speed of the individual particles that propagate in the structure. The transmission of any physical quantity in a waveguide is not connected with phase speed. It is related to the wavenumber through the relation

$$C_{ph} = \mathrm{Re}\left(\frac{\Omega_1}{\alpha_j}\right). \tag{26}$$

During the propagation of waves, group of particles are travelled in bundles. The speed of each bundle is called the group speed. This is the velocity of energy transport, and it must be constrained. It is mathematically expressed as

$$C_{gr} = \mathrm{Re}\left(\frac{\partial\Omega_1}{\partial\alpha_j}\right). \tag{27}$$

## The DSM Method Formulation

### DSM of *j*th Segment

The boundary conditions for dimensionless axial displacement and axial force of *j*th segment can be expressed as:

At $x_j = 0 (i.e., \xi_j = 0)$, $U_j = U_{1_j}$ and $N_j = -N_{1_j}$

At $x_j = L_j (i.e., \xi_j = 1)$, $U_j = U_{2_j}$ and $N_j = N_{2_j}$

Substituting the boundary conditions into Eqs. (22, 23) to obtain the displacements and forces vectors respectively as:

$$\begin{bmatrix} U_{1_j} \\ U_{2_j} \end{bmatrix} = \begin{bmatrix} 1 & 0 \\ \cos(\alpha_j) & \sin(\alpha_j) \end{bmatrix} \begin{bmatrix} C_{1j} \\ C_{2j} \end{bmatrix}, \tag{28}$$

$$\begin{bmatrix} N_{1_j} \\ N_{2_j} \end{bmatrix} \left( \frac{L}{E_1 A_1} \right) = \gamma_j \alpha_j \begin{bmatrix} 0 & -1 \\ -\sin(\alpha_j) & \cos(\alpha_j) \end{bmatrix} \begin{bmatrix} C_{1j} \\ C_{2j} \end{bmatrix}. \tag{29}$$

The displacements and forces vectors may be expressed respectively as:

$$\mathbf{U}_j = \mathbf{A}_j \mathbf{C}_j, \tag{30}$$

$$\mathbf{F}_j = \mathbf{B}_j \mathbf{C}_j = \mathbf{D}_j \mathbf{U}_j, \tag{31}$$

where,

$$\mathbf{D}_j = \mathbf{B}_j \mathbf{A}_j^{-1} = \begin{bmatrix} D_j(1,1) & D_j(1,2) \\ D_j(2,1) & D_j(2,2) \end{bmatrix} \tag{32}$$

and $\mathbf{D}_j$ is the DSM of $j$th segment without attachments.

### The Overall DSM

The overall DSM for all the system (stepped nanorod embedded in various elastic media with different boundary conditions) may be obtained as:

$$\mathbf{D} = \begin{bmatrix} D_1(1,1) & D_1(1,2) & 0 & 0 & 0 \\ D_1(2,1) & D_1(2,2) + D_2(1,1) & : & 0 & 0 \\ 0 & : & : & : & 0 \\ 0 & 0 & : & D_{J-1}(2,2) + D_J(1,1) & D_J(1,2) \\ 0 & 0 & 0 & D_J(2,1) & D_J(2,2) \end{bmatrix} + \mathbf{S} \tag{33}$$

where $\mathbf{S}$ is the overall dimensionless attachments matrix in diagonal form as:

$$\mathbf{S} = \begin{bmatrix} \bar{K}_{s_1} & 0 & 0 & 0 & 0 \\ 0 & 0 & 0 & 0 & 0 \\ 0 & 0 & \ddots & 0 & 0 \\ 0 & 0 & 0 & 0 & 0 \\ 0 & 0 & 0 & 0 & \bar{K}_{s_{J+1}} \end{bmatrix} \tag{34}$$

where $\bar{K}_{s1} = \frac{K_{s1} E_1 A_1}{L}$ and $\bar{K}_{s(J+1)} = \frac{K_{s(J+1)} E_1 A_1}{L}$ are the left and right linear dimensionless stiffness respectively.

The overall DSM is function of the dimensionless natural frequency parameters $\Omega_1$. Newton–Raphson method is used to solve the DSM in Eq. (33). The solution is obtained by using very small initial guess $\Omega_0 = 10^{-9}$ and using incremental step of $\Omega_{inc} = 0.001$. The roots of this equation are the dimensionless natural frequency parameters $\Omega_1$.

## Results and Discussions

This section is divided into three subsections. The first subsection describes a two-segment rod model. The second subsection includes some verification results which are selected from literature to verify the results of the present model. The third subsection includes some new results obtained using the present model.

### Two-Segment Nanorod Embedded in Two Different Elastic Media

Figure 2 shows two-segment nanorod made from the same material ($E_{21} = \rho_{21} = 1$) and embedded in two different elastic media. The dimensionless elastic media stiffness of the 1st and 2nd segment are $\bar{K}_1$ and $\bar{K}_2 = K_{21}\bar{K}_1$ respectively. The first and second segment dimensionless length are $l_1$ and $l_2 = 1 - l_1$ respectively. The dimensionless attached springs stiffness at the left and right are denoted by $\bar{K}_{s_1}$ and $\bar{K}_{s_3}$, respectively. $A_{21}$ is the ratio of the second to the first cross sectional area.

### Verification of Results

***Example 1*** This example presents the analysis of two-segment nanorod with two different cross-sectional areas. The ratio $A_{21}$ equals to 2, and there is no surrounding elastic media ($\bar{K}_1 = \bar{K}_2 = 0$ and $K_{21} = 1$). The analysis is carried out at nanorod with total length $L = 25$ nm. The effects of the first step location$l_1 = [0.01{:}0.99]$ and the nonlocal parameter $e_0 a = [0\ \ 0.2\ \ 0.5]$ nm are investigated. C–C ($K'_{s_1} = K'_{s_3} = \infty$) and C–F ($K'_{s_1} = \infty$ and $K'_{s_3} = 0$)

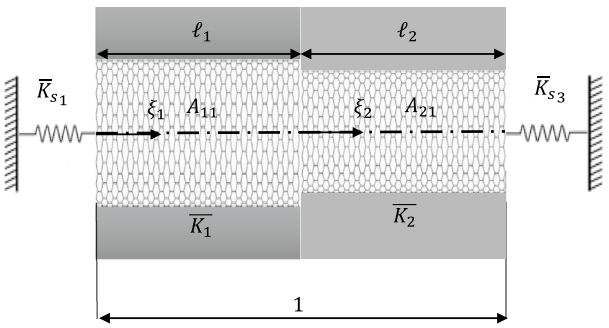


**Fig. 2** Two-segment nanorod embedded in two different elastic media

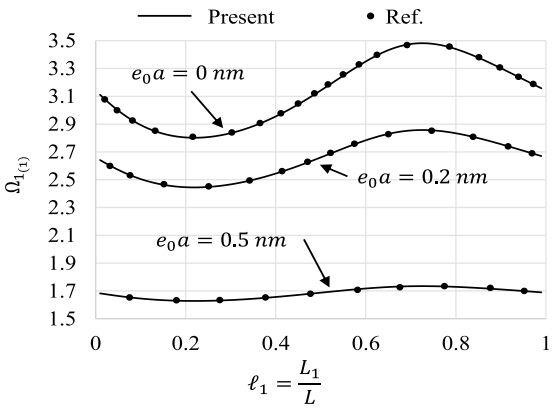


**Fig. 3** The first dimensionless natural frequency for C–C rod

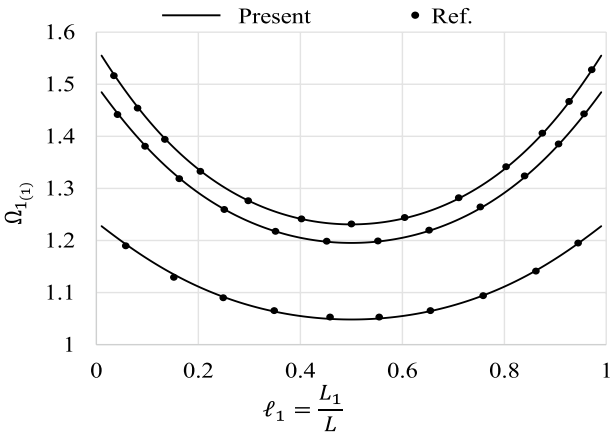


**Fig. 4** The first dimensionless natural frequency for C–F rod

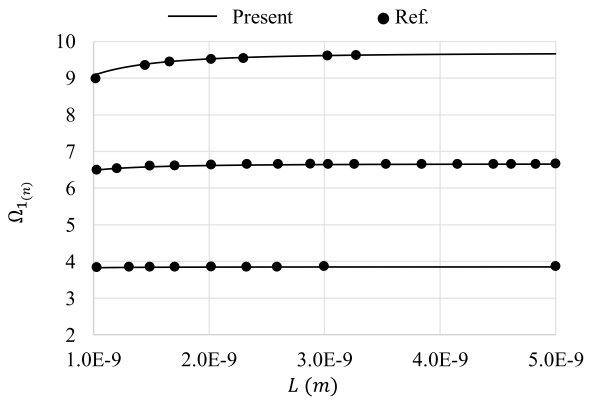


**Fig. 5** The first three dimensionless natural frequency for C–C rod

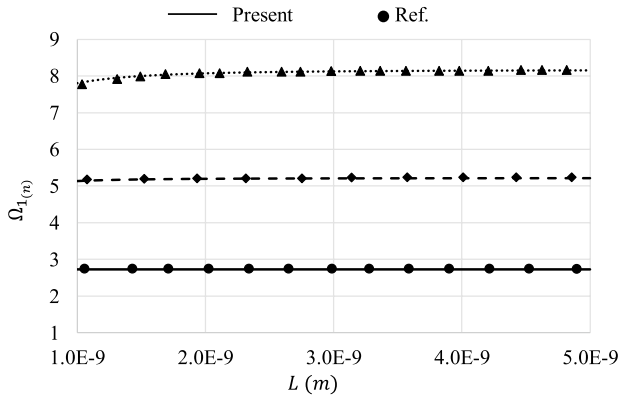


**Fig. 6** The first three dimensionless natural frequency for C–F rod

boundary conditions are investigated and compared with the results presented in [24].

Figures 3 and 4 show the first dimensionless natural frequency $\Omega_{1_{(1)}}$ for C–C and C–F rod respectively. Figure 3 shows that $\Omega_{1_{(1)}}$ decreases through the first quarter of step location and then increases through the second and third quarter then return to decreasing by going to the end. Figure 4 shows that $\Omega_{1_{(1)}}$ decreases through the first half of the step location ratio and return to increase by going to the end. It can be seen that the results are in good agreement with Loghmani, Yazdi [24] results.

***Example 2*** This example studies a uniform rod ($A_{21} = 1$) that is fully embedded in one elastic medium ($K_{21} = 1$). Clamped-clamped ($K'_{s_1} = K'_{s_3} = \infty$ ) and C–F ($K'_{s_1} = \infty$ and $K'_{s_3} = \infty$ ) are investigated and compared with the solution presented in [22]. The analysis is carried out at $\bar{K}_1 = 5, e_0a = \frac{0.1421}{\sqrt{12}}$ nm. Also, the variation of nanorod length $L = 1{:}5$ nm is examined.

Figures 5 and 6 show the first three dimensionless natural frequencies for C–C and C–F rod respectively for different lengths. The two figures indicate that with increasing the nanorod length the scale effect decreases, and the results close to the classical effect. From the figure results, It can be seen that the results are in good agreement with the results of Gul et al. [22].

## New Results of the Present Model

### Spectrum and Dispersion Relations for a Uniform Rod Partially Embedded in an Elastic Media

A uniform rod ($A_{21} = 1$) partially embedded in an elastic media ($K_{21} = 0$) is investigated. The total length of nanorod $L = 25$ nm and the two-segment length ratio are ($l_1 = 0.25$

and $l_2 = 0.75$). The analysis is carried out at $\bar{K}_1 = 10$ for $e_0a = [0, 0.5, 1]$ nm.

The spectrum and dispersion curves obtained from local ($e_0a = 0$) and nonlocal rod model for the two segments of the rod are shown in Figs. 7 and 8. Figure 7 shows the variation of the nondimensional wavenumbers with nondimensional wave frequencies for both local and nonlocal theories. From this figure, the waves start propagating in the second segment at any excitation frequency and does not have a cut-off frequency, unlike the first segment, the waves start propagation at a certain frequency called cut-off frequency. The cut-off frequencies are independent of the nonlocal parameter and directly proportional to the elastic media stiffness. In the present study and for the first segment, the nondimensional cut-off frequency is at 3.1623 for both local and nonlocal theories.

For the case of local theory ($e_0a = 0$), the wavenumbers increase linearly with the nondimensional frequency for the second segment as shown in Fig. 7 . This linear variation denotes that the waves will propagate in nondispersive mode (i.e., the waves do not change their shapes as they propagate) as shown in Fig. 8, where the group speed is constant with the increase in frequency. Also, the wavenumbers increase monotonically for first segment with the increase in frequency and correspondingly, the group speed increase with increase in wave frequency. However, at higher frequencies, the group speeds attain a constant

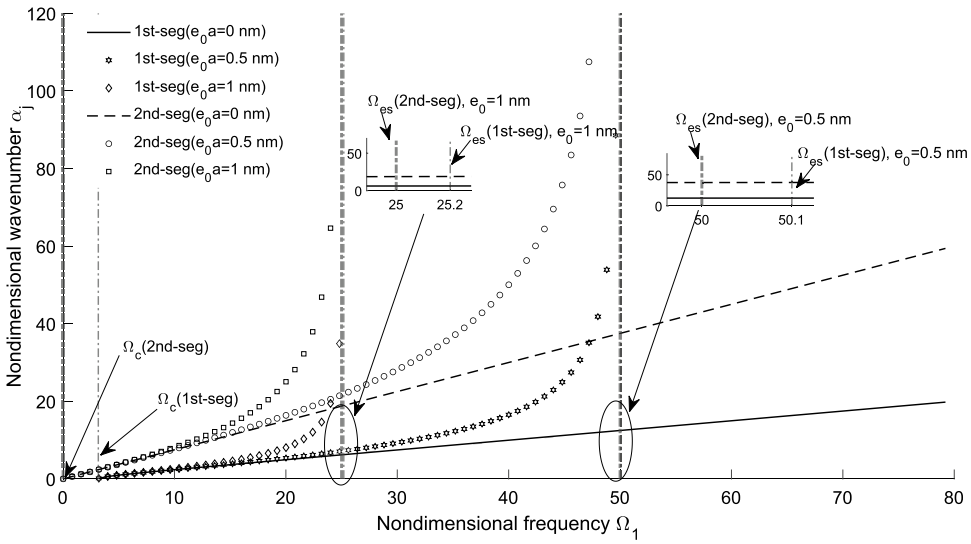


**Fig. 7** Spectrum relation for different nonlocal parameters

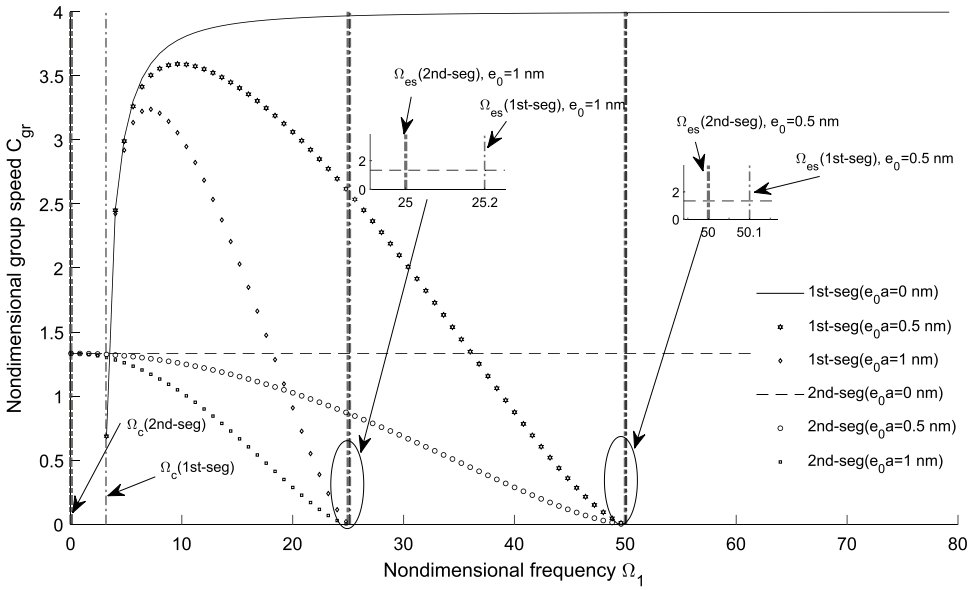


**Fig. 8** Group speed dispersion relation for different nonlocal parameters

value. On the other hand, with the introduction of nonlocal parameter, the wave behavior is completely changed. For both segments the wavenumbers have a nonlinear variation with frequency, which indicates that the waves are dispersive in nature. Also, the wavenumbers tend to infinity at a certain frequency called escape frequency and after this frequency there is no wave propagation. The escape frequencies are inversely proportional to the nonlocal parameter and directly proportional to the elastic media stiffness. In the present case for the first segment, the nondimensional escape frequency is at 50.0999 and 25.1992 and for second segment is at 50.0 and 25.0 for $e_0a = 0.5$ and 1 nm, respectively.

### Uniform Rod Embedded in Two Different Elastic Media

A uniform rod ($A_{21} = 1$) embedded in two different elastic media is investigated. The total length of nanorod $L = 25$ nm and the two-segment are equal ($l_1 = l_2 = 0.5$). The analysis is carried out at $e_0a = 0.5{:}2$ nm, $K_{21} = 0{:}5$ and $\bar{K}_1 = 0{:}10$.

*Clamped-clamped rod* In the case of C–C rod and for free vibration analysis, the stiffness of the boundary springs takes the following values: $\bar{K}s_1 = \bar{K}s_3 = \infty$.

Figure 9 shows the first and second dimensionless natural frequencies of C–C rod for different nonlocal parameters at (a, b, c and d). It shows that with increasing $\bar{K}_1$ or $K_{21}$ the natural frequency increases. Figure 9a–d show

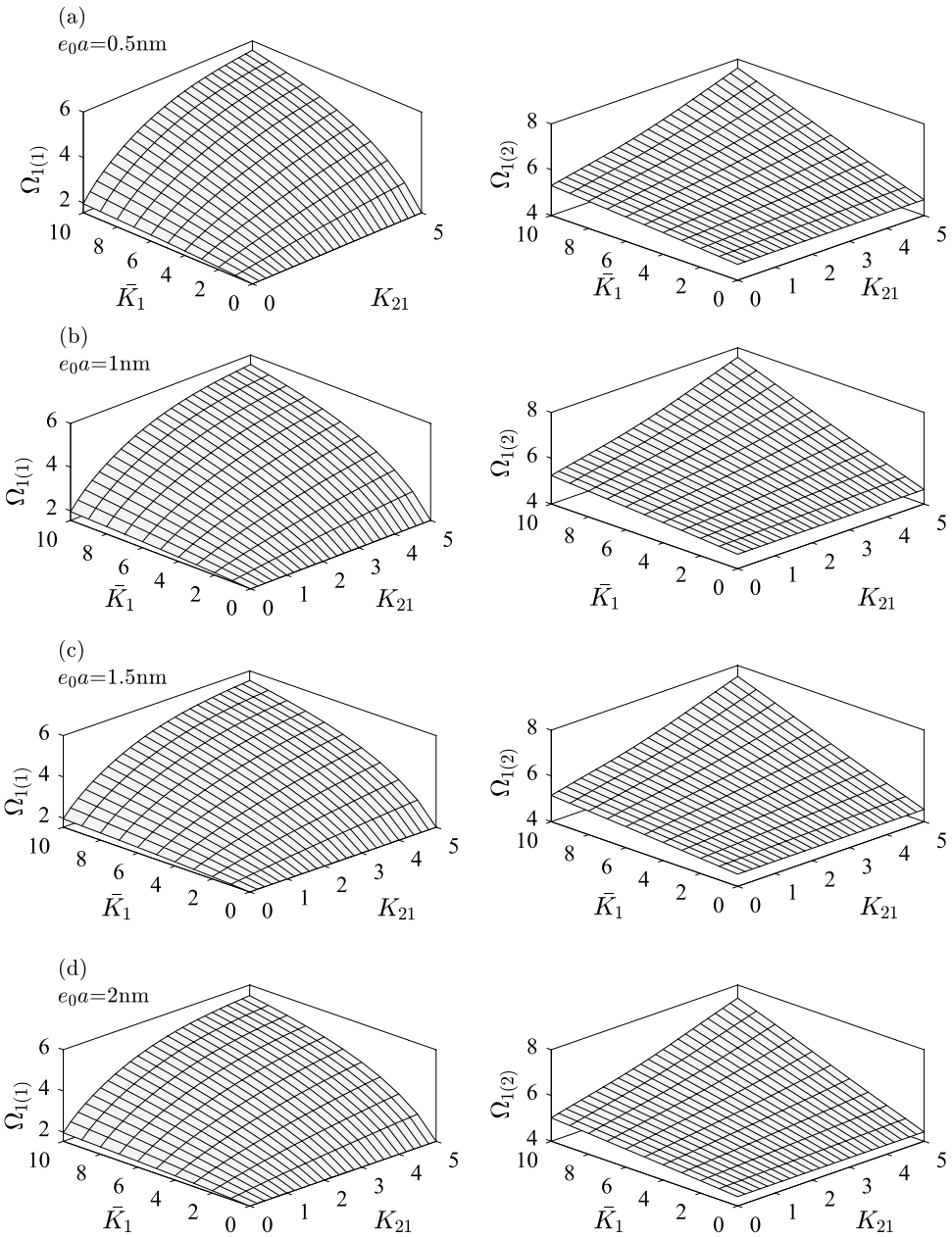


**Fig. 9** The first and second dimensionless natural frequency for C–C rod

that with increasing the nonlocal parameter the natural frequency in both 1st mode and 2nd mode decreases.

Table 1 shows the first five dimensionless natural frequencies for C–C rod at different nonlocal parameters $e_0a, \bar{K}_1$ and $K_{21}$. The table results show that increasing the values of $\bar{K}_1$, $K_{21}$, results in an increase in the dimensionless natural frequencies. By increasing$e_0a$, the dimensionless natural frequencies decrease in all modes however the decrease is a slightly bigger in the higher modes.

*Clamped-free rod* In the case of clamped-free boundary conditions the input values for the rod end conditions become as follows: $\bar{K}s_1 = \infty$ and $\bar{K}s_3 = 0$.

**Table 1** First five natural frequencies for C–C rod

| Clamped-clamped rod | | | | | | | | | |
|---|---|---|---|---|---|---|---|---|---|
| $e_0a = 0.5$ nm | | | | | $e_0a = 0.5$ nm | | | | |
| $\bar{K}_1$ | | 2 | 5 | 10 | | | 2 | 5 | 10 |
| $K_{21}$ | $n$ | | | | | n | | | |
| 0.5 | 1 | 3.3646 | 3.6793 | 4.1434 | 0.5 | 1 | 3.3475 | 3.6636 | 4.1291 |
| | 2 | 6.3525 | 6.5291 | 6.8166 | | 2 | 6.2148 | 6.3952 | 6.6882 |
| | 3 | 9.3406 | 9.46 | 9.6555 | | 3 | 8.9022 | 9.0274 | 9.2318 |
| | 4 | 12.2466 | 12.3384 | 12.4903 | | 4 | 11.293 | 11.3924 | 11.5565 |
| | 5 | 15.0333 | 15.1079 | 15.2313 | | 5 | 13.3553 | 13.4392 | 13.5777 |
| 1 | 1 | 3.439 | 3.8506 | 4.4527 | 1 | 1 | 3.4223 | 3.8357 | 4.4399 |
| | 2 | 6.3914 | 6.6219 | 6.9893 | | 2 | 6.2546 | 6.49 | 6.8644 |
| | 3 | 9.3673 | 9.5261 | 9.785 | | 3 | 8.9302 | 9.0967 | 9.3675 |
| | 4 | 12.267 | 12.3887 | 12.5888 | | 4 | 11.315 | 11.4468 | 11.6632 |
| | 5 | 15.05 | 15.1493 | 15.3134 | | 5 | 13.3741 | 13.4858 | 13.6699 |
| 2 | 1 | 3.5779 | 4.1434 | 4.9194 | 2 | 1 | 3.5618 | 4.1291 | 4.9063 |
| | 2 | 6.4706 | 6.8166 | 7.3693 | | 2 | 6.3354 | 6.6882 | 7.2497 |
| | 3 | 9.4204 | 9.6555 | 10.0336 | | 3 | 8.9859 | 9.2318 | 9.626 |
| | 4 | 12.3079 | 12.4903 | 12.7903 | | 4 | 11.3593 | 11.5565 | 11.8792 |
| | 5 | 15.0831 | 15.2313 | 15.4748 | | 5 | 13.4113 | 13.5777 | 13.8498 |
| $e_0a = 1.5$ nm | | | | | $e_0a = 2$ nm | | | | |
| $\bar{K}_1$ | | 2 | 5 | 10 | | | 2 | 5 | 10 |
| $K_{21}$ | $n$ | | | | | n | | | |
| 0.5 | 1 | 3.319732 | 3.637996 | 4.105913 | 0.5 | 1 | 3.282192 | 3.603507 | 4.07456 |
| | 2 | 6.004947 | 6.191208 | 6.492895 | | 2 | 5.745523 | 5.939616 | 6.25239 |
| | 3 | 8.293825 | 8.427996 | 8.646293 | | 3 | 7.623707 | 7.769288 | 8.004982 |
| | 4 | 10.10755 | 10.21827 | 10.40023 | | 4 | 8.94591 | 9.070322 | 9.273089 |
| | 5 | 11.49586 | 11.5931 | 11.753 | | 5 | 9.856991 | 9.970024 | 10.15475 |
| 1 | 1 | 3.395204 | 3.811484 | 4.418983 | 1 | 1 | 3.358562 | 3.778881 | 4.390893 |
| | 2 | 6.046093 | 6.289296 | 6.674971 | | 2 | 5.788574 | 6.042151 | 6.442638 |
| | 3 | 8.323987 | 8.50228 | 8.791403 | | 3 | 7.656542 | 7.850009 | 8.162269 |
| | 4 | 10.13225 | 10.27923 | 10.51962 | | 4 | 8.973904 | 9.139526 | 9.409088 |
| | 5 | 11.51762 | 11.64713 | 11.85983 | | 5 | 9.882407 | 10.03304 | 10.2792 |
| 2 | 1 | 3.535571 | 4.105913 | 4.884926 | 2 | 1 | 3.50019 | 4.07456 | 4.856002 |
| | 2 | 6.129582 | 6.492895 | 7.0677 | | 2 | 5.875486 | 6.25239 | 6.843321 |
| | 3 | 8.383548 | 8.646293 | 9.06478 | | 3 | 7.721122 | 8.004982 | 8.453132 |
| | 4 | 10.1815 | 10.40023 | 10.75501 | | 4 | 9.029087 | 9.273089 | 9.66275 |
| | 5 | 11.5608 | 11.753 | 12.06507 | | 5 | 9.932532 | 10.15475 | 10.51095 |

Where $n$ is the mode index

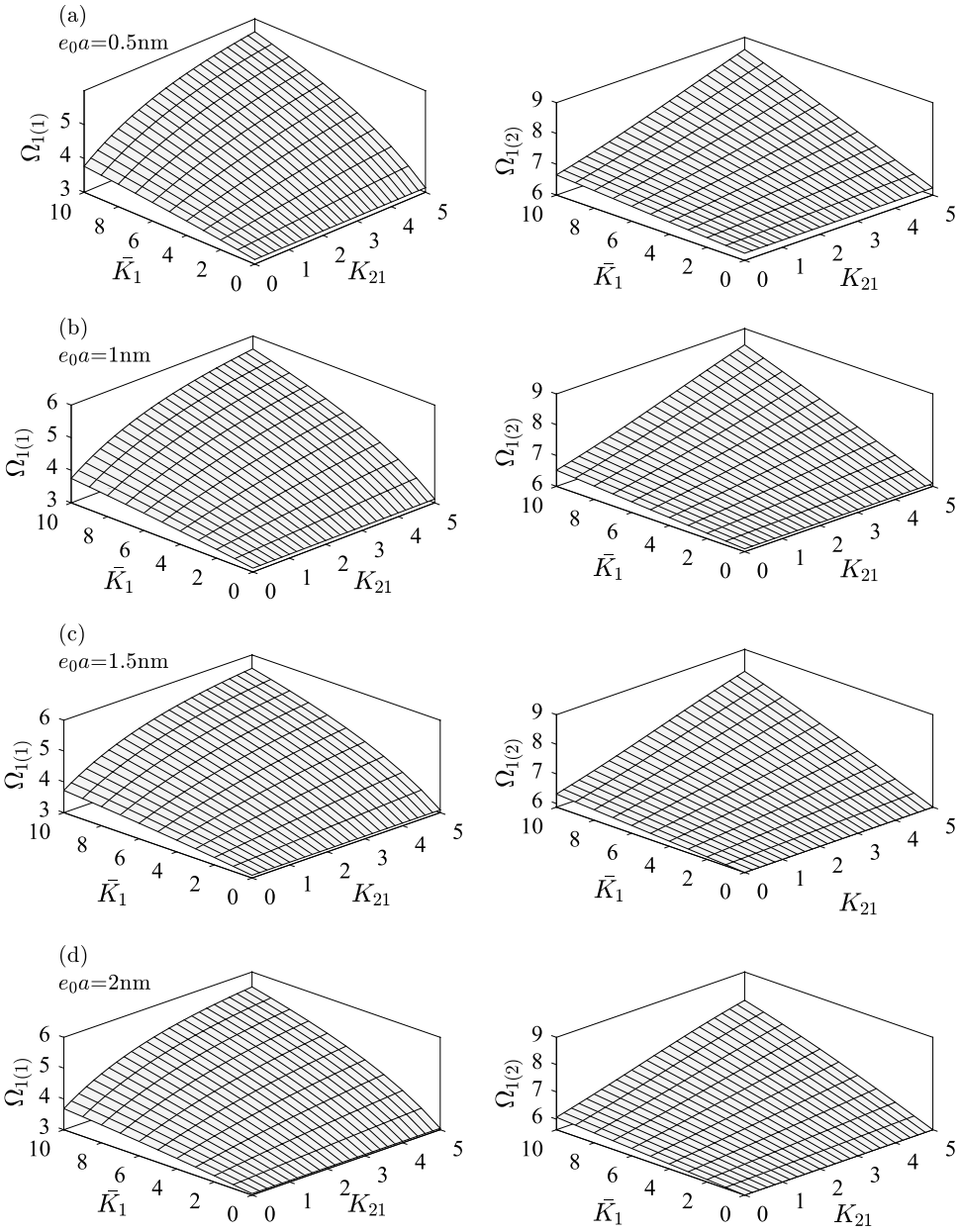


**Fig. 10** The first and second dimensionless natural frequency for C–F rod

Figure 10 shows the first and second dimensionless natural frequencies of C–F rod for different nonlocal parameters at (a, b, c and d).

Table 2 shows the first five dimensionless natural frequencies for clamped-free rod at different nonlocal parameters $e_0a, \bar{K}_1$ and $K_{21}$. Table 2 and Figure 10 show that the dimensionless natural frequency increases with the increase in the of $\bar{K}_1 or K_{12}$. The subfigures (a, b, c and d) show that with increasing the nonlocal parameter, the natural frequency in both modes decreases. However, the trend of changing the natural frequency with $\bar{K}_1, K_{12}$ and $e_0a$ is the same for both C–C and C–F boundary conditions.

## Conclusions

The natural frequencies of a stepped rod embedded in several elastic media and for different boundary conditions are introduced in the present work. Dynamics stiffness matrix method and Eringen's theory are used for this analysis. Two cases from the literature are used to validate the present model. Then,a selected case of two-segment nanorod embedded in two elastic media is deeply investigated. The effects of varying the nonlocal parameter and stiffness of elastic media and its ratio were considered. The spectrum and dispersion relations were obtained for partially embedded nanorod. The results show that the

**Table 2** First five natural frequencies for C–F rod

| Clamped-free rod | | | | | | | | |
|---|---|---|---|---|---|---|---|---|
| $e_0a = 0.5$ nm | | | | | $e_0a = 0.5$ nm | | | |
| $\bar{K}_1$ | | 2 | 5 | 10 | | 2 | 5 | 10 |
| $K_{21}$ | $n$ | | | | n | | | |
| 0.5 | 1 | 1.9083 | 2.3212 | 2.873 | 0.5 | 1 | 1.9068 | 2.3206 | 2.8731 |
| | 2 | 4.8594 | 5.102 | 5.4835 | | 2 | 4.8002 | 5.0447 | 5.4288 |
| | 3 | 7.8504 | 7.9871 | 8.2105 | | 3 | 7.5884 | 7.7304 | 7.9622 |
| | 4 | 10.8095 | 10.9161 | 11.0915 | | 4 | 10.1401 | 10.2528 | 10.4379 |
| | 5 | 13.6566 | 13.7372 | 13.8705 | | 5 | 12.3652 | 12.4548 | 12.6027 |
| 1 | 1 | 2.1129 | 2.7321 | 3.5305 | 1 | 1 | 2.1112 | 2.7308 | 3.5295 |
| | 2 | 4.8997 | 5.1968 | 5.6575 | | 2 | 4.8416 | 5.142 | 5.6072 |
| | 3 | 7.8859 | 8.0739 | 8.3778 | | 3 | 7.6246 | 7.8189 | 8.1323 |
| | 4 | 10.8307 | 10.9683 | 11.1939 | | 4 | 10.1632 | 10.3098 | 10.5495 |
| | 5 | 13.676 | 13.7852 | 13.9654 | | 5 | 12.3862 | 12.5067 | 12.705 |
| 2 | 1 | 2.4651 | 3.376 | 4.4656 | 2 | 1 | 2.4628 | 3.3731 | 4.4612 |
| | 2 | 4.9809 | 5.3913 | 6.0313 | | 2 | 4.9248 | 5.3408 | 5.988 |
| | 3 | 7.9569 | 8.2468 | 8.7093 | | 3 | 7.6969 | 7.9943 | 8.4671 |
| | 4 | 10.8731 | 11.073 | 11.3995 | | 4 | 10.2094 | 10.4233 | 10.7715 |
| | 5 | 13.7147 | 13.8812 | 14.1546 | | 5 | 12.4279 | 12.6098 | 12.9071 |
| $e_0a = 1.5$ nm | | | | | $e_0a = 2$ nm | | | |
| $\bar{K}_1$ | | 2 | 5 | 10 | | 2 | 5 | 10 |
| $K_{21}$ | $n$ | | | | n | | | |
| 0.5 | 1 | 1.9045 | 2.3194 | 2.8732 | 0.5 | 1 | 1.9012 | 2.3179 | 2.8732 |
| | 2 | 4.7065 | 4.9543 | 5.3422 | | 2 | 4.5849 | 4.837 | 5.2301 |
| | 3 | 7.2062 | 7.3567 | 7.6014 | | 3 | 6.7597 | 6.921 | 7.1821 |
| | 4 | 9.26 | 9.3821 | 9.5818 | | 4 | 8.3463 | 8.4802 | 8.6979 |
| | 5 | 10.8498 | 10.9524 | 11.1212 | | 5 | 9.4441 | 9.5623 | 9.7549 |
| 1 | 1 | 2.1084 | 2.7286 | 3.5278 | 1 | 1 | 2.1044 | 2.7255 | 3.5254 |
| | 2 | 4.7497 | 5.0556 | 5.528 | | 2 | 4.6304 | 4.9437 | 5.4259 |
| | 3 | 7.2436 | 7.4478 | 7.7762 | | 3 | 6.7986 | 7.0158 | 7.3635 |
| | 4 | 9.286 | 9.4462 | 9.7072 | | 4 | 8.376 | 8.5532 | 8.8406 |
| | 5 | 10.8731 | 11.0102 | 11.2349 | | 5 | 9.4704 | 9.6275 | 9.8838 |
| 2 | 1 | 2.4589 | 3.3683 | 4.4538 | 2 | 1 | 2.4536 | 3.3616 | 4.4435 |
| | 2 | 4.8361 | 5.2611 | 5.9196 | | 2 | 4.7211 | 5.158 | 5.831 |
| | 3 | 7.3179 | 7.6273 | 8.1159 | | 3 | 6.8757 | 7.2004 | 7.7083 |
| | 4 | 9.3377 | 9.5727 | 9.9522 | | 4 | 8.4345 | 8.6948 | 9.11 |
| | 5 | 10.9194 | 11.1237 | 11.4548 | | 5 | 9.5222 | 9.7529 | 10.1223 |

Where $n$ is the mode index

start of wave propagation is independent of the nonlocal parameter but depends on the surrounded elastic media stiffness.

In local theory, the waves propagate in nondispersive mode with constant speed for the segment without surrounding elastic media. Unlike the other segment with surrounding elastic media, the group speed increase with frequency to attain a constant value. In the nonlocal theory, the waves propagate in dispersive mode from the cut-off frequency to the escape frequency where the wave speed reaches zero. The escape frequencies are inversely proportional to the nonlocal parameter and directly proportional to the elastic media stiffness.

The dimensionless natural frequencies were obtained for C–C and C–F rod. The present results indicate that increasing the elastic media stiffness and its ratio, increase the dimensionless natural frequencies. Also, increasing nonlocal parameter decreases the dimensionless natural frequencies except for some points at the first mode of C–F boundary conditions. This decrease is more remarkable at the higher modes. The present results may be of great benefit in evaluating nanobeam elastic modulus based on the measurement of its resonance.

**Funding** The authors declares that they do not receive any fund for this work



## References

1. Karlicic D, Murmu T, Adhikari S, McCarthy M (2015) Non-local structural mechanics. Wiley, New York. https://doi.org/10.1002/9781118572030.ch2
2. Iijima S (1991) Helical microtubules of graphitic carbon. Nature 354(6348):56. https://doi.org/10.1038/354056a0
3. Hancock Y (2011) The 2010 nobel prize in physics-ground-breaking experiments on graphene. J Phys D Appl Phys 44(47):473001. https://doi.org/10.1088/0022-3727/44/47/473001
4. Tang C, Meng L, Sun L, Zhang K, Zhong J (2008) Molecular dynamics study of ripples in graphene nanoribbons on 6 h-sic (0001): temperature and size effects. J Appl Phys 104(11):113536. https://doi.org/10.1063/1.3032895
5. Murmu T, Adhikari S (2012) Nonlocal frequency analysis of nanoscale biosensors. Sens Actuators A 173(1):41–48. https://doi.org/10.1016/j.sna.2011.10.012
6. Andrianov IV, Awrejcewicz J (2004) Theory of plates and shells: new trends and applications. Int J Nonlinear Sci Numer Simul 5(1):23–36. https://doi.org/10.1515/IJNSNS.2004.5.1.23
7. Bauer S, Pittrof A, Tsuchiya H, Schmuki P (2011) Size-effects in tio2 nanotubes: diameter dependent anatase/rutile stabilization. Electrochem Commun 13(6):538–541. https://doi.org/10.1016/j.elecom.2011.03.003
8. Eringen AC (1972) Nonlocal polar elastic continua. Int J Eng Sci 10(1):1–16. https://doi.org/10.1016/0020-7225(72)90070-5
9. Gopalakrishnan S, Narendar S (2013) Wave propagation in nanostructures: nonlocal continuum mechanics formulations. Springer, Berlin
10. Reddy J (2007) Nonlocal theories for bending, buckling and vibration of beams. Int J Eng Sci 45(2–8):288–307. https://doi.org/10.1016/j.ijengsci.2007.04.004
11. Şimşek M, Yurtcu H (2013) Analytical solutions for bending and buckling of functionally graded nanobeams based on the nonlocal timoshenko beam theory. Compos Struct 97:378–386. https://doi.org/10.1016/j.compstruct.2012.10.038
12. Eltaher MA, Mohamed NA (2020) Vibration of nonlocal perforated nanobeams with general boundary conditions. Smart Struct Syst 25(4):501–514. https://doi.org/10.12989/sss.2020.25.4.501
13. Taima MS, El-Sayed TA, Farghaly SH (2020) Free vibration analysis of multistepped nonlocal Bernoulli–Euler beams using dynamic stiffness matrix method. J Vib Control. https://doi.org/10.1177/1077546320933470
14. Behdad S, Fakher M, Hosseini-Hashemi S (2021) Dynamic stability and vibration of two-phase local/nonlocal vfgp nanobeams incorporating surface effects and different boundary conditions. Mech Mater. https://doi.org/10.1016/j.mechmat.2020.103633
15. Aydogdu M (2009) Axial vibration of the nanorods with the nonlocal continuum rod model. Phys E 41(5):861–864. https://doi.org/10.1016/j.physe.2009.01.007
16. Huang Z (2012) Nonlocal effects of longitudinal vibration in nanorod with internal long-range interactions. Int J Solids Struct 49(15–16):2150–2154. https://doi.org/10.1016/j.ijsolstr.2012.04.020
17. Aydogdu M (2012) Axial vibration analysis of nanorods (carbon nanotubes) embedded in an elastic medium using nonlocal elasticity. Mech Res Commun 43:34–40. https://doi.org/10.1016/j.mechrescom.2012.02.001
18. Adhikari S, Murmu T, McCarthy M (2013) Dynamic finite element analysis of axially vibrating nonlocal rods. Finite Elem Anal Des 63:42–50. https://doi.org/10.1016/j.finel.2012.08.001
19. Demir C (2013) Civalek, Torsional and longitudinal frequency and wave response of microtubules based on the nonlocal continuum and nonlocal discrete models. Appl Math Model 37(22):9355–9367. https://doi.org/10.1016/j.apm.2013.04.050
20. Guüven U (2014) Love-bishop rod solution based on strain gradient elasticity theory. Comptes Rendus Méc 342(1):8–16. https://doi.org/10.1016/j.crme.2013.10.011
21. Adhikari S, Murmu T, McCarthy M (2014) Frequency domain analysis of nonlocal rods embedded in an elastic medium. Phys E 59:33–40. https://doi.org/10.1016/j.physe.2013.11.001
22. Gul U, Aydogdu M, Gaygusuzoglu G (2016) Axial dynamics of a nanorod embedded in an elastic medium using doublet mechanics. Compos Struct. https://doi.org/10.1016/j.compstruct.2016.11.023
23. Numanoğlu HM, Akgöz B, Civalek O (2018) On dynamic analysis of nanorods. Int J Eng Sci 130:33–50. https://doi.org/10.1016/j.ijengsci.2018.05.001
24. Loghmani M, Yazdi MRH, Bahrami MN (2018) Longitudinal vibration analysis of nanorods with multiple discontinuities based on nonlocal elasticity theory using wave approach. Microsyst Technol 24(5):2445–2461. https://doi.org/10.1007/s00542-017-3619-y
25. Ebrahimi F, Barati MR, Civalek, (2019) Application of Chebyshev–Ritz method for static stability and vibration analysis of nonlocal microstructure-dependent nanostructures. Eng Comput. https://doi.org/10.1007/s00366-019-00742-z
26. Civalek O, Uzun B, Yaylı MO, AkgÖz B (2020) Size-dependent transverse and longitudinal vibrations of embedded carbon and silica carbide nanotubes by nonlocal finite element method. Eur Phys J Plus 135(4):381. https://doi.org/10.1140/epjp/s13360-020-00385-w

27. Yayli M (2020) Axial vibration analysis of a Rayleigh nanorod with deformable boundaries. Microsyst Technol. https://doi.org/10.1007/s00542-020-04808-7
28. El-Sayed TA, Farghaly SH (2016) Exact vibration of timoshenko beam combined with multiple mass spring sub-systems. Struct Eng Mech 57(6):989–1014
29. El-Sayed TA, Farghaly SH (2020) Formulae for the frequency equations of beam-column system carrying a fluid storage tank. Struct Eng Mech 73(1):83–95. https://doi.org/10.12989/sem.2020.73.1.083
30. El-Sayed TA, Farghaly S (2016) Exact free vibration analysis of timoshenko stepped shaft carrying elastically supported eccentric masses with application on swro mechanical system. Desalination 385:194–206. https://doi.org/10.1016/j.desal.2016.02.010
31. Farghaly SH, El-Sayed TA (2016) Exact free vibration of multi-step timoshenko beam system with several attachments. Mech Syst Signal Process 72:525–546. https://doi.org/10.1016/j.ymssp.2015.11.025
32. El-Sayed TA, El-Mongy H (2019) Free vibration and stability analysis of a multi-span pipe conveying fluid using exact and variational iteration methods combined with transfer matrix method. Appl Math Model 71:173–193. https://doi.org/10.1016/j.apm.2019.02.006
33. El-Sayed TA, Farghaly SH (2017) A normalized transfer matrix method for the free vibration of stepped beams: comparison with experimental and fe (3d) methods. Shock Vib. https://doi.org/10.1155/2017/8186976
34. Williams F, Wittrick W (1970) An automatic computational procedure for calculating natural frequencies of skeletal structures. Int J Mech Sci 12(9):781–791. https://doi.org/10.1016/0020-7403(70)90053-6
35. Banerjee J (1997) Dynamic stiffness formulation for structural elements: a general approach. Comput Struct 63(1):101–103. https://doi.org/10.1016/S0045-7949(96)00326-4
36. El-Ella M, El-Sayed TA, Farghaly S (2018) Vibration and stability analysis of pipe conveying fluid using dynamic stiffness matrix and numerical methods
37. Harland NR, Mace BR, Jones RW (2001) Wave propagation, reflection and transmission in tunable fluid-filled beams. J Sound Vib 241(5):735–754. https://doi.org/10.1006/jsvi.2000.3316
38. Mei C, Karpenko Y, Moody S, Allen D (2006) Analytical approach to free and forced vibrations of axially loaded cracked timoshenko beams. J Sound Vib 291(3):1041–1060. https://doi.org/10.1016/j.jsv.2005.07.017
39. Mei C (2012) Wave analysis of in-plane vibrations of l-shaped and portal planar frame structures. J Vib Acoust 134:2. https://doi.org/10.1115/1.4005014
40. Mei C, Sha H (2016) Analytical and experimental study of vibrations in simple spatial structures. J Vib Control 22(17):3711–3735. https://doi.org/10.1177/1077546314565807
41. Eringen AC (1983) On differential equations of nonlocal elasticity and solutions of screw dislocation and surface waves. J Appl Phys 54(9):4703–4710. https://doi.org/10.1063/1.332803